33RD CONGRESS
OF THE INTERNATIONAL COUNCIL
OF THE AERONAUTICAL SCIENCES
STOCKHOLM, SWEDEN, 4-9 SEPTEMBER, 2022

ICAS 2022 SWEDEN

EFFECTIVENESS ANALYSIS OF DOBC Q-FILTER PARAMETERS FOR A MULTICOPTER UAV

Hoijo Jeaong[1], Chisung Roh[1], Yeonghwan Jang[1], Jinyoung Suk*[1] & Seungkeun Kim[1]

[1]Department of Aerospace Engineering, Chungnam National University

Abstract

In this study, the parameters of the Q-filter for the disturbance observer (DOB)-based controller are selected through simulation and verified through experiment. The Q-filter is a low pass filter (LPF) designed to allow DOB to estimate disturbance in a wide frequency range. However, bandwidth is a significant variable that determines the robustness and the effect on the noise of the system. The limitation of robustness due to the Q-filter design directly affects the tracking performance of the DOB-based control system. The robustness and stability of the system can be guaranteed by estimating and eliminating disturbances through an appropriate Q-filter design. In this study, the relevant parameters of the Q-filter are selected through a nonlinear model of multicopter built based on a wind tunnel test. Furthermore, an indoor experiment of the motion capture environment is performed to verify the Q-filter parameters obtained from the simulation. The step or doublets are commanded for different magnitudes and durations to obtain the Q-filter parameters' performance validation.

Keywords: Multicopter, aerodynamic database, disturbance observer, experiment, motion capture system, doublet motion, Q-filter

1. Introduction

Multicopter systems are sensitive to disturbance due to their trade-offs in mechanical simplicity compared to efficient aerodynamic design and the complexity of rotor systems similar to fixed-wing and helicopters [1, 2]. In particular, wind disturbance is an essential issue for multicopter safety and mission in the performance of complicated urban terrain and bad weather condition. To solve this problem, many control methods have been used to design various aircraft control systems, including linear and nonlinear control methods. In [3], To control the altitude and speed, disturbance observer based control (DOBC) are designed by applying irregular disturbances to the longitudinal modeling of a fixed-wing aircraft. To cope with various disturbance conditions, nonlinear dynamic inversion (NDI) is combined with DOBC. In [4], to analyze the control recovery performance of the multicopter nominal model, DOBC is used as a central controller. The manipulator is combined to compare the control effectiveness through trajectory following flight. In addition, there are studies on DOBC compensating for uncertain parameters in disturbance conditions [5] and trajectory control using a disturbance observer with finite-time convergence (FTDO) for coaxial helicopter UAVs [6].

In previous studies, the fidelity between simulation and flight experiments is not guaranteed because the dynamic modeling of the target system is simplified. In addition, the controller design parameters are different between simulation and flight tests, making it challenging to apply to existing systems. In addition, in terms of DOBC, there is no trial and error method for optimally designing control the Q filter.

Motivated by the discussions mentioned above, this paper performs dynamic modeling of the multicopter based on a wind tunnel test, verifies the robust control improvement through simulation and the experiment. The contributions of this paper are summarized:

1. Numerical modeling of the multicopter UAV is performed based on a wind tunnel test.

2. The control performance of the DOBC is analyzed using simulation and indoor experimental according to Q filter τ.

Section 2 presents the modeling of a multicopter based on a wind tunnel test. In Section 3, the DOBC design is done using the nominal model of the multicopter. After that, the simulation results are shown in Section 4 according to τ. In Section 5, attitude control performance is analyzed through experiments using an indoor motion capture system. Finally, Section 6 concludes this paper.

2. Dynamic modeling

2.1 Design of aerodynamic database

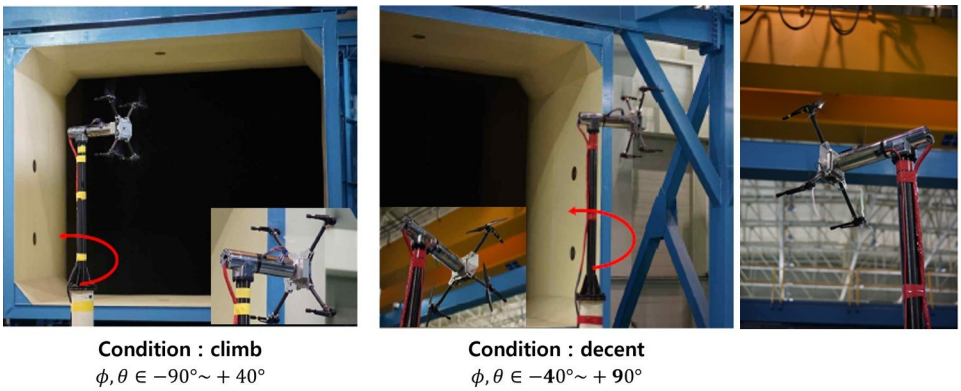

Figure 1 – Wind tunnel test of the multicopter

An aerodynamic database is constructed using the wind tunnel data of the multicopter performed by the Korea Aerospace Research Institute (KARI) to build a dynamics model. As shown in Figure 1, these data are acquired according to angle of attack $-90° \sim 90°$, flight speed $0 \sim 15 m/s$, and RPM range $0 \sim 6000\,RPM$.

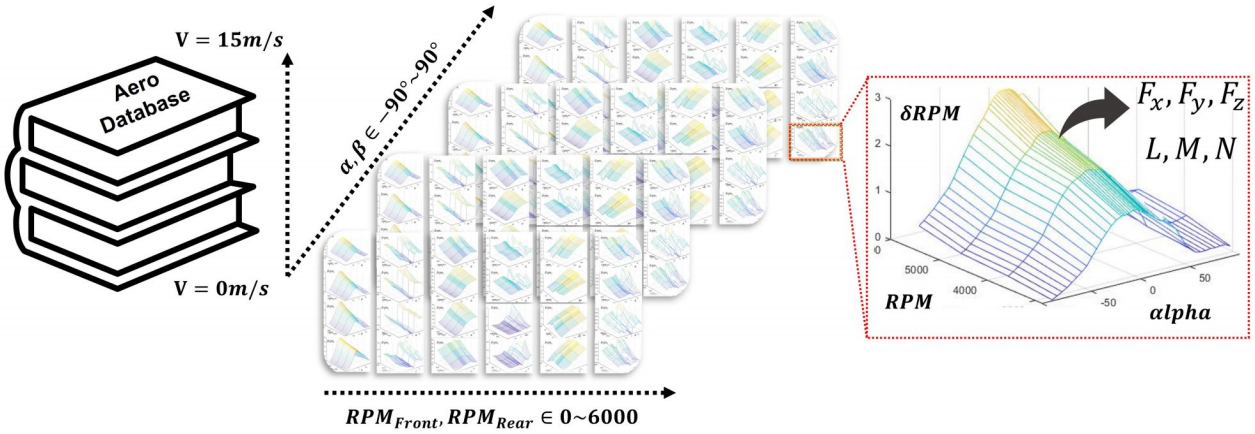

Figure 2 – Aerodynamic lookup table structure

In order to simultaneously consider the forward and lateral speeds, the angle of attack, the lateral angle, and the rotational speed of the four motors, an aerodynamic table should be constructed in an additional way. This study constructs the aerodynamic lookup tables as a database, as shown in Figure 2. The database is interpolated by wind speeds as a three-dimensional space composed of aerodynamic tables according to angles of attack and lateral angles. The amount of change in rotational speed δRPM is used to construct the aerodynamic table corresponding to each motor. Corresponding to the flight conditions and the four control surfaces, the forces and moments are provided.

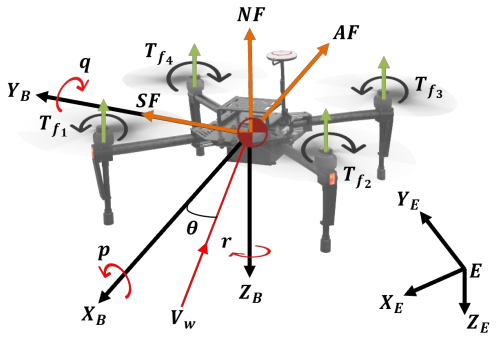

Figure 3 – The coordinate system of a multicopter

2.2 System dynamics

Figure 3 shows the body-fixed coordinate of the multicopter. A conventional north-east-down (NED) earth fixed inertial frame of reference is taken, where the frame's origin is a local position at the starting moment. The aircraft's orientation can be described by integrating Z-Y-X consecutive rotations of the Euler rate in terms of the angular body rates [7, 8, 9] as follows:

$$\begin{pmatrix} \dot{\phi} \\ \dot{\theta} \\ \dot{\psi} \end{pmatrix} = \begin{pmatrix} 1 & \tan\theta\sin\phi & \tan\theta\cos\phi \\ 0 & \cos\phi & -\sin\phi \\ 0 & \sin\phi\cos\theta & \cos\phi\cos\theta \end{pmatrix} \begin{pmatrix} p \\ q \\ r \end{pmatrix}. \tag{1}$$

The kinematic relationship for the translational motion of the inertial frame in terms of body-fixed frame velocity can be described as follows:

$$\begin{pmatrix} \dot{x}_i \\ \dot{y}_i \\ \dot{z}_i \end{pmatrix} = \begin{pmatrix} c\theta c\psi & c\phi s\theta c\phi - c\phi s\psi & c\phi s\theta c\psi + s\phi s\psi \\ c\theta s\psi & s\phi s\theta s\psi + c\phi c\psi & c\phi s\theta s\psi - s\phi c\psi \\ -s\theta & s\theta s\theta & c\phi c\theta \end{pmatrix} \begin{pmatrix} u \\ v \\ w \end{pmatrix} \tag{2}$$

where c and s denote the cosine and sine; $x, y, \& z$ represent the multicopter's inertial position, $\phi, \theta, \& \varphi$ are the roll, pitch, and yaw angles.
The positions in the inertial frame can be described by integrating (2). A general six degrees of freedom translation and the rotational dynamics of the aerial system in the body-fixed frame can be modeled as follows:

$$\begin{aligned} \dot{u} &= vr - wq + F_x/m \\ \dot{v} &= wp - ur + F_y/m \\ \dot{w} &= uq - vp + F_z/m \\ \dot{p} &= \{qr(J_{yy} - J_{zz}) + L\}/J_{xx} \\ \dot{q} &= \{pr(J_{zz} - J_{xx}) + M\}/J_{yy} \\ \dot{r} &= \{pqJ_{xx} - J_{yy}) + N\}/J_{zz} \end{aligned} \tag{3}$$

where F_x, F_y, and F_z are external forces; L, M, and N are external moments; u, v, and w refers to translational velocity in the body-fixed frame; and p, q, and r refers to rotational velocity in the body-fixed frame. J_{xx}, J_{yy}, and J_{zz} denotes the mass moment of inertia, which is calculated using computer aided design (CAD). Cross products are neglected because they are trivial for miniature scale systems.

3. Control design

A block diagram of the disturbance observer is shown in Figure 4. $P(s)$ is the actual system with uncertainties and a single-input single-output (SISO) minimum phase transfer function, while u_p and y are the input and output of the system, respectively. $C(s)$ is the outer loop controller based on PID, which is either designed for the nominal system $P_n(s)$, or designed to track the reference input r for

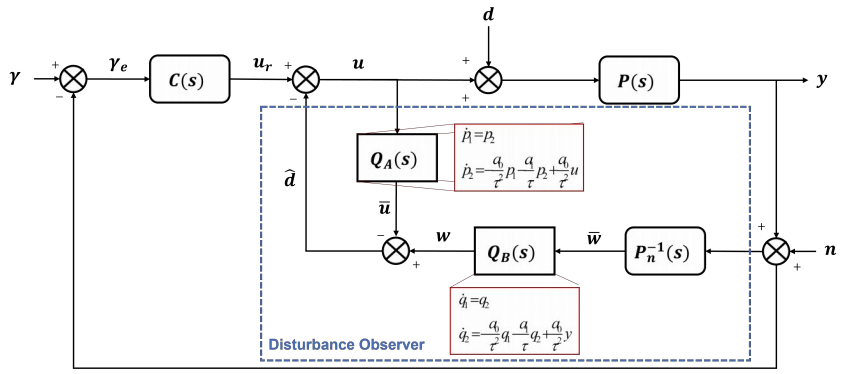

Figure 4 – The block diagram of the disturbance observer

an actual system, without considering disturbances and plant uncertainty. The actual SISO system can be expressed as the following state-space representation [10]:

$$\dot{x} = f(x) + gu + gd. \tag{4}$$

The actual system $P(s)$ is uncertain; therefore, a robust controller design is required. The nominal system $P_n(s)$ can be expressed as follows:

$$\dot{x} = f_n(x) + g_n\bar{u} \tag{5}$$

where $\bar{u}$ is the external control input from the outer-loop controller. The desired control input can be selected so that the closed-loop system from (4) becomes equivalent to the nominal system (5) as:

$$u_{desired} = -d + \frac{1}{g}\{-f(x) + f_n(x)\} + \frac{g_n}{g}\bar{u}. \tag{6}$$

This is not directly feasible because the actual system is uncertain $f(x)$, g, and d are unknown. However, it has been demonstrated that the underlying dynamics of $Q_A(s)$ estimate $u_{desired}$. Conceptually, the disturbance observer is intended to estimate the input to the system, including disturbance u_p using the inverse of the nominal model $P_n^{-1}(s)$. Then, the outer-loop controller output u_r is subtracted. This becomes the estimated disturbance $\hat{d}$, which is formulated as follows:

$$u = \bar{u} + u_r - \hat{u}_p = \bar{u} - \hat{d}. \tag{7}$$

The estimated disturbance $\hat{d}$ can be represented from Figure 4 as follows:

$$\hat{d} = Q_B(s)P_n(s)^{-1}y - Q_A(s)u \tag{8}$$

where $Q_A(s)$ and $Q_B(s)$ are referred to as Q-filters, which enable the realization of the inverse of the nominal plant. The Q-filters are conventionally taken as stable low pass filters, with the DC gain set as unity to satisfy $\lim_{\omega\to 0} Q(j\omega) = 1$ for the exact disturbance estimate. In addition, they should have more relative degrees than the nominal system, to make the transfer function of the inverse of the nominal system realizable. In conventional designs, the Q-filters are taken as a stable low pass filter:

$$Q_A(s) = Q_B(s) = \frac{c_{\mu-1}(\tau s)^{\mu-1} + \cdots + c_1(\tau s) + c_0}{(\tau s)^{\mu} + a_{\mu-1}(\tau s)^{\mu-1} + \cdots + a_0} \tag{9}$$

It is not easy to select the proper parameters of the Q-filter for a nonlinear system. This study analyzes the control performance according to the Q-filter design variables while applying step and doublet attitude inputs to reliable multicopter modeling based on wind tunnel test data. Moreover, to analyze the simulation results and the actual multicopter flight test tendency, an indoor flight test environment is established to confirm the effect of the Q-filter design parameters.

4. Numerical Simulation

In this study, the performance of the proposed control algorithm is demonstrated through a numerical simulation. The value required for numerical modeling of the multicopter is referred to as [12]. The initial conditions of all states are zero, $p = q = r = \dot{z} = 0$. The roll and pitch angle commands are applied simultaneously in the hovering flight in this simulation. For simulation study, the harmonic disturbance is given below

$$\begin{aligned} d_x(t) &= \frac{1}{\tau_x}\sin(\omega_x t)J_{xx}, \\ d_y(t) &= \frac{1}{\tau_y}\sin(\omega_y t)J_{yy}, \end{aligned} \tag{10}$$

where τ_x and τ_y decide the amplitude of the disturbance; ω_x and ω_y represent the frequency of the disturbance. Using these design parameters of the DOBC controller, the multicopter numerical model is simulated in MATLAB, considering the disturbance. To analyze the effectiveness of the proposed control algorithm, each simulation is run for $60\,s$.

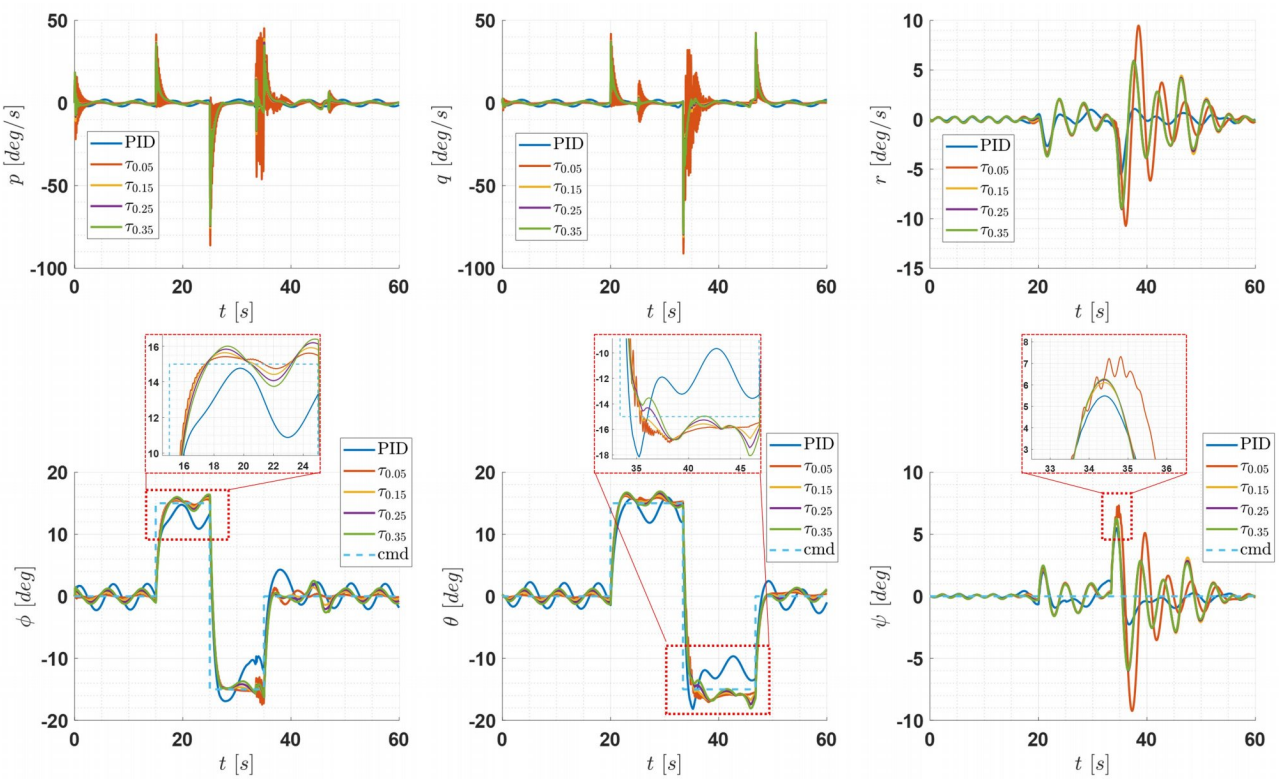

Figure 5 – State responses in the disturbance.

The primary design parameter of DOBC's Q filter is τ, because the tuning of the Q filter changes the following performance against disturbance and the control robustness. To compare the controller performance according to τ, PID and DOBC are applied, as shown in Figure 5. τ is changed from 0.05 to 0.35, and the attitude and angular velocity results are presented. Due to disturbances irregularly applied to the multicopter x and y axes, the overall attitude tracking result is the same as a sine wave. In particular, the PID vibrates the most and does not follow the doublet command. Conversely, noise or overshoot increases when $\tau = 0.05$ and $\tau = 0.35$. The Q filter needs tuning depending on the control target and environment, and in particular, τ seems to have a significant influence on the attitude tracking error.

Figure 6 shows the disturbance estimation result. If τ is small when the system is noisy or there is much noise in the disturbance, the estimation of the disturbance is not clean. Especially, $\tau = 0.05$ shows extensive noisy disturbance estimation at $20\,s$ and $38\,s$ in the roll and pitch axis. Due to this effect, the yaw axis is vibrated up to 12° degrees. Conversely, $\tau = [0.15, 0.25]$ correctly estimates the disturbance and compensates the controller.

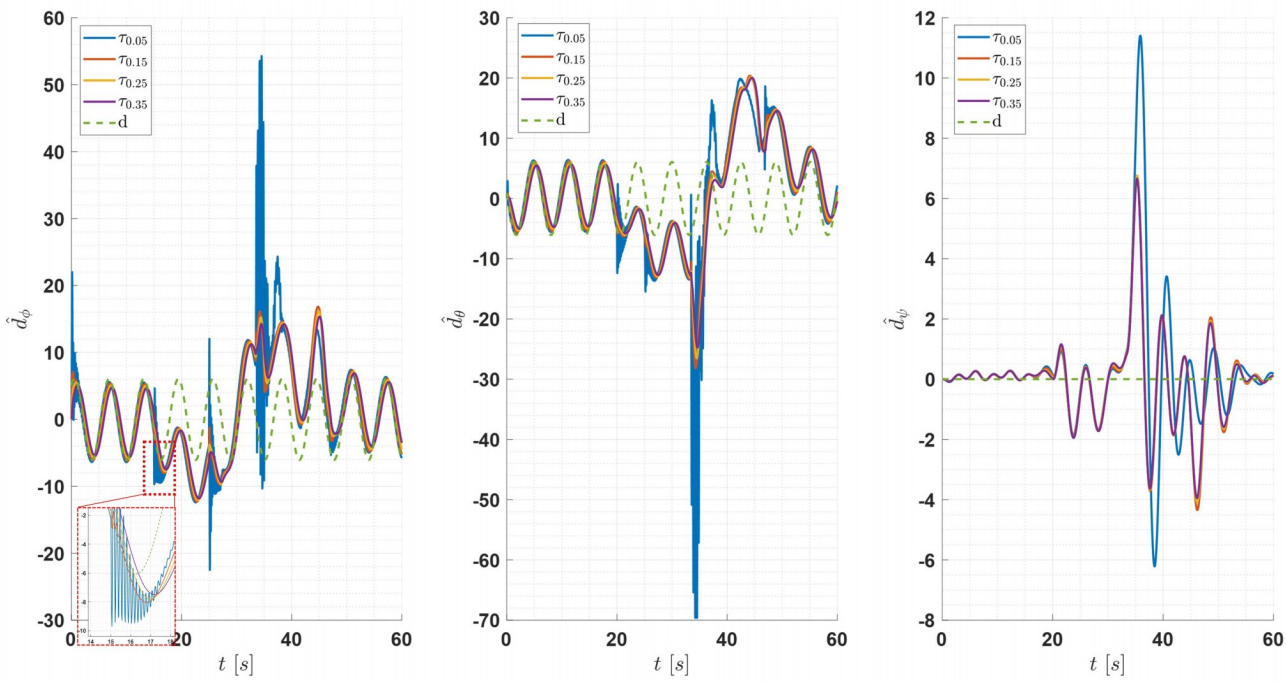

Figure 6 – Estimation of disturbance results in the disturbance.

Table 1 – RMSE of the simulation

ϕ	**PID**	$\tau = 0.05$	$\tau = 0.15$	$\tau = 0.25$	$\tau = 0.35$
RMSE	3.242°	2.785°	2.841°	2.950°	3.055°
θ	**PID**	$\tau = 0.05$	$\tau = 0.15$	$\tau = 0.25$	$\tau = 0.35$
RMSE	3.055°	2.767°	2.764°	2.783°	2.830°

Root mean square error (RMSE) is calculated in Table 1 to compare control effectiveness. Although the performance difference is not significant in the RMSE, when analyzed with Figures 5 and 6, τ shows satisfactory control performance from 0.15 to 0.25. In particular, PID does not show the most significant RMSE value for the doublet command. This implies that control effectiveness is improved by using DOBC for time-varying disturbance.

5. Experiment

In this study, a DJI MATRICE 100 multicopter is modified to fly in an indoor environment, as shown in Figure 7. An Intel NUC with an i7 processor and a pixhawk are used for a mission computer and a flight control computer, respectively. In order to fly in an indoor environment where GPS signals are not available, IR markers for motion capture are installed asymmetrically on the multicopter as shown Figure 7(a). Indoor motion capture camera data in Figure 7(b) is transmitted to the mission computer based on network communication, and the flight control computer conducts indoor positioning based on the navigation information.

The electric fan is installed diagonally to the multicopter to create an irregular disturbance. The multicopter is mounted on the testbed and freely moved by ball bearings. To compare the performance of the controller, the doublet command is given to the flight control computer to analyze the result under the same conditions according to τ.

Figure 8 shows the multicopter system constructed in this study. The position and attitude signals of the synchronized IR markers from the 14 motion capture cameras are transmitted to the companion computer through Ethernet communication. At the same time, the T265 tracking camera also estimates the position and attitude of the multicopter. The companion computer communicates with the ground control system (GCS) through Wifi, and the flight control computer transmits and receives data using the MAVROS communication protocol through USB. The position and attitude data output from the indoor test's motion capture system is calculated again through the flight control computer's

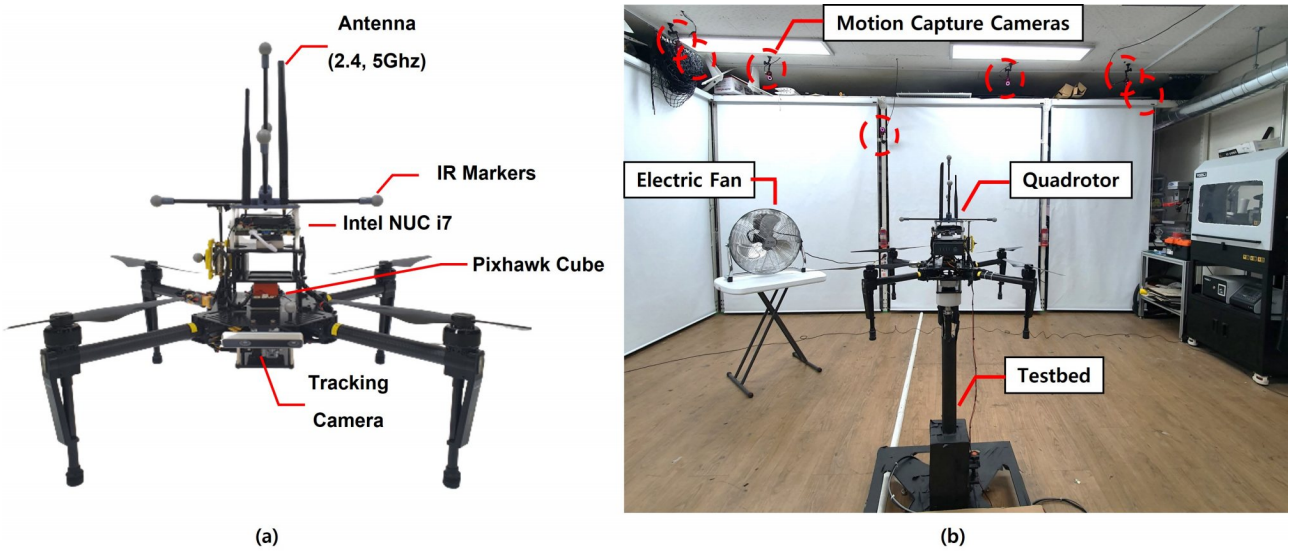

Figure 7 – Manufactured multicopter (a) and indoor flight test environment (b)

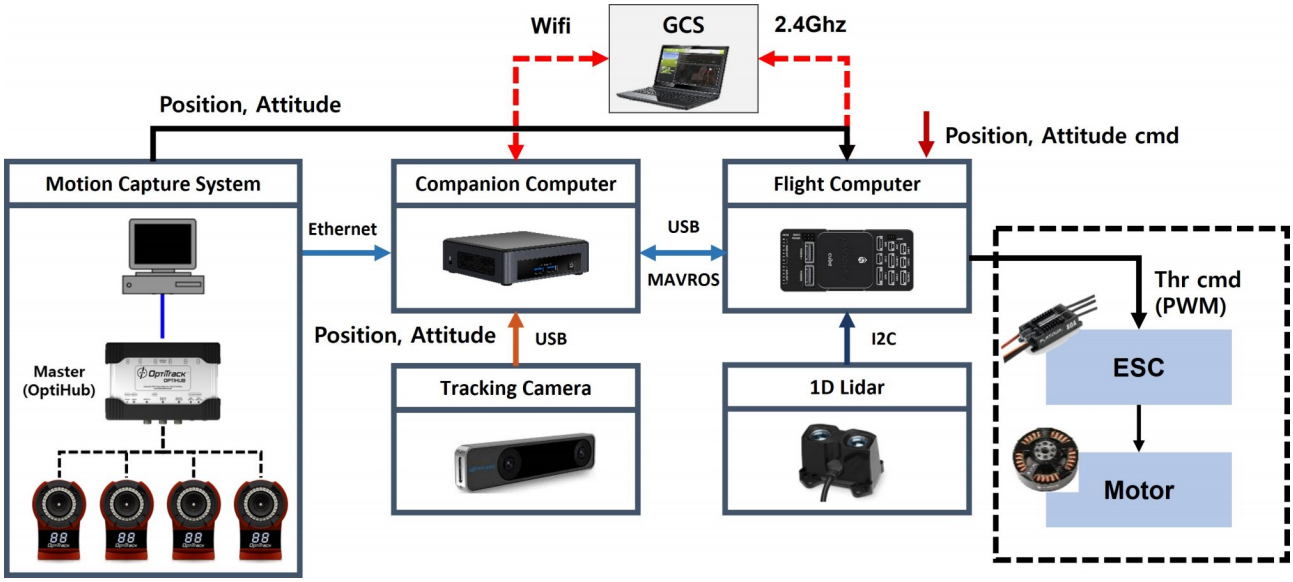

Figure 8 – Multicopter System Configuration

extended Kalman filter (EKF) through coordinate transformation.

Figure 9 is a comparison of control performance for disturbance according to τ. The experiment's inevitable overshoot and undershoot effects are observed using the testbed. The center of gravity of the multicopter manufactured is located at the top, and the ball bearing of the testbed is located at the bottom. Like simulation, PID has a slow convergence speed and tends to overshoot. In particular, the roll angle does not maintain 0° in the $15s$ and $20s$. Similarly, at $\tau = 0.05$, the undershoot is the largest due to the noisy disturbance estimate. Table 2 shows the RMSE of attitude tracking according to τ. As with the simulation trend, PID shows high error, and $\tau = 0.05$ shows the highest error due to noisy characteristics and undershoot. However, as shown in Figure 9, the convergence speed is the fastest in $\tau = 0.05$. Conversely, if τ is raised to 0.65, there is little difference in performance, but it is thought that if a disturbance in a high-frequency band on the system, the control effectiveness will decrease. Both simulation and experiment show a small attitude error at $\tau = 0.35$. In the case of the multicopter manufactured in this paper, it can be seen that the current disturbance and system guarantee the disturbance estimation performance and control effectiveness when τ is 0.35.

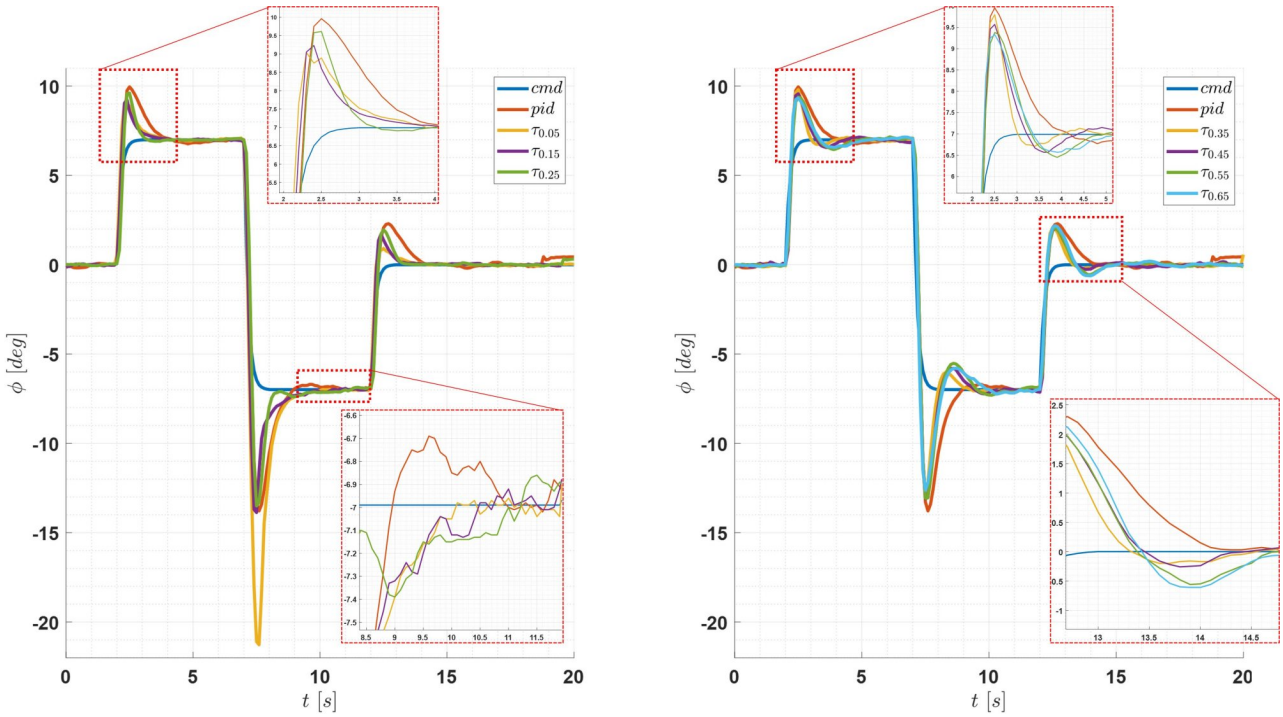

Figure 9 – Response to doublet input of roll axis according to τ

Table 2 – RMSE of the ground test

	PID	$\tau = 0.05$	$\tau = 0.15$	$\tau = 0.25$
RMSE	1.409°	2.1662°	1.136°	1.138°
	$\tau = 0.35$	$\tau = 0.45$	$\tau = 0.55$	$\tau = 0.65$
RMSE	1.066°	1.159°	1.191°	1.138°

6. Conclusion and Ongoing Work

In this study, a parametric study is performed on the design of a Q-filter that comprises a disturbance observer. The closed-loop characteristics may change depending on the Q-filter variables, and the position or attitude tracking performance may vary significantly. In this study, the control performance according to the change of Q-filter variables will be finally analyzed through the multicopter modeling and experiment.

In a future study, we will analyze the flight performance by installing a manipulator on the bottom of a multicopter equipped with a DOBC controller in an indoor motion capture system environment.

7. Contact Author Email Address

mailto: jsuk@cnu.ac.kr (corresponding author)
mailto: jeaonghoijo@cnu.ac.kr

8. Copyright Statement

Acknowledgements

This work was supported by the Korea Evaluation Institute of Industrial Technology(KEIT) grant funded by the Korea government(MTIE) (No.20016775).

This work was supported by the National Research Foundation of Korea(NRF) grant funded by the Korea government(MSIT) (No. NRF-2021R1A2C2013363).

This work was supported by the National Research Foundation of Korea(NRF) grant funded by the Korea government(MSIT)(No. 2021R1A5A1031868).

References

[1] Michael, Nathan, et al., "The grasp multiple micro-uav testbed," IEEE Robotics & Automation Magazine, vol. 17, no. 3, pp. 56-65, 2010.

[2] Kumar, Vijay, and Nathan Michael., "Opportunities and challenges with autonomous micro aerial vehicles," The International Journal of Robotics Research, vol. 31, no. 11, pp. 1279-1291, 2012.

[3] Liu, Cunjia, and Wen-Hua Chen., "Disturbance rejection flight control for small fixed-wing unmanned aerial vehicles," Journal of Guidance, Control, and Dynamics, vol. 39, no. 12, pp. 2810-2819, 2016.

[4] Kim, S., Choi, S., Kim, H., Shin, J., Shim, H., and Kim, H. J., "Robust control of an equipment-added multirotor using disturbance observer," IEEE Transactions on Control Systems Technology, vol. 26, no. 4, pp, 1524-1531, 2017.

[5] Benevides, J. R., Paiva, M. A., Simplício, P. V., Inoue, R. S., and Terra, M. H., "Disturbance Observer-based Robust Control of a Quadrotor Subject to Parametric Uncertainties and Wind Disturbance," IEEE Access, 2022.

[6] Mokhtari, M. Rida, Brahim Cherki, and Amal Choukchou Braham., "Disturbance observer based hierarchical control of coaxial-rotor UAV," ISA transactions, vol. 67, pp. 466-475, 2017.

[7] Nelson, Robert C., "Flight stability and automatic control," vol. 2, New York: WCB/McGraw Hill, 1998.

[8] P. Pounds, R. Mahony and P. Corke., "Modelling and control of a large quadrotor robot", Control Engineering Practice, vol. 18, no. 7, pp. 691-699, 2010.

[9] R. Mahony, V. Kumar and P. Corke, "Multirotor aerial vehicles: Modeling estimation and control of quadrotor," Robotics Automation Magazine IEEE, vol. 19, no. 3, pp. 20-32, 2012.

[10] Shim, Hyungbo, and Young-Jun Joo., "State space analysis of disturbance observer and a robust stability condition," 46th IEEE Conference on Decision and Control, IEEE, 2007.

[11] Li, Shihua, et al, "Disturbance observer-based control: methods and applications," CRC press, 2014.

[12] Jeaong, H., Jo, S., Suk, J., Kim, S., Lee, Y., and Chung, I., "Modeling of aerodynamic database and robust control using disturbance observer for quadcopter," Journal of Institute of Control, Robotics and Systems, vol. 24, no. 6, pp. 519-531, 2018.